

## Sierpiński Pyramids by Molecular Entanglement

Rajarshi Sarkar, Ting-Zheng Xie, Kevin J. Endres, Zilu Wang, Charles N. Moorefield, Mary Jane Saunders, Suman Ghorai, Anil K. Patri, Chrys Wesdemiotis,\* Andrey V. Dobrynnin,\* and George R. Newkome\*



Cite This: *J. Am. Chem. Soc.* 2020, 142, 5526–5530



Read Online

ACCESS |

Metrics & More

Article Recommendations

Supporting Information

**ABSTRACT:** Planar, terpyridine-based metal complexes with the Sierpiński triangular motif and alkylated corners undergo a second self-assembly event to give megastructural Sierpiński pyramids; assembly is driven by the facile lipophilic–lipophilic association of the alkyl moieties and complementary perfect fit of the triangular building blocks. Confirmation of the 3D, pyramidal structures was verified and supported by a combination of TEM, AFM, and multiscale simulation techniques.

Nature has evolved over millions of years to present design principles for the self-assembly of objects of specific size, shape, and functionality using proteins as building blocks. Some viruses that infect Archaea (a separate kingdom of life between bacteria and eukaryotes) induce the formation of micromolar 7-fold rotationally symmetrical pyramid structures [virus-associated pyramids (VAPs)] from a single 10 kDa protein (PVAP) in the archaeal plasma membrane that creates 100 nm windows allowing the mature virus to escape. This supramolecular assembly requires one in-plane interaction within the triangular facets and one out-of-plane interaction at the edges of the pyramid from a single protein.<sup>1–3</sup> The proteins' 3D structure controls the pathways and robustness of the self-assembly process. Development of synthetic analogues of the protein-like assembly for the generation of precisely ordered, functional materials has the potential to develop new classes of designer materials with a high degree-of-structural-purity that could have impact in such areas as metamaterials,<sup>4,5</sup> nonlinear optics,<sup>6,7</sup> energy and nanoscale devices,<sup>8</sup> molecular encapsulation,<sup>9</sup> and “smart” materials applications.<sup>10–14</sup>

A fundamental tenet underpinning these and other applications involves the ease-of-construction associated with single-step, high yield, and well-defined assembly protocols. The recently reported self-assembly of otherwise difficult-to-obtain materials (Figure 1), possessing diverse, structurally precise, and well-defined motifs has been demonstrated by (1) incorporation of supporting strategic functionalities and sites-of-connectivity within monomers leading to an overall quantitative conversion;<sup>15,16</sup> (2) use of exact stoichiometry with regard to polyfunctional monomers leading to precision construction;<sup>17</sup> (3) logical matching of preassembled building blocks that can facilitate the generation of complex multi-metallomaterials through multicomponent disassembly and rearrangement;<sup>18,19</sup> and (4) balance of metal connectivity, coordination directivity, and external parameters (e.g., temperature, concentration, etc.) resulting in architecturally different assemblies. These concepts provide a multidivergent foundation regarding the ability to craft designer nano- and macromolecular materials.<sup>20</sup>

As the construction of target structures becomes more predictable, but also more complex, it was beneficial to use monomers that possess  $-\text{OCH}_3$ <sup>21,22</sup> or  $-\text{F}$ <sup>23,24</sup> tags to help confirm the symmetry of the resultant product(s) using  $^1\text{H}$  or  $^{19}\text{F}$  NMR or to change the localized electron demand.<sup>24</sup> Since these intermediates need to be totally soluble throughout the self-assembly process, use of lipophilic  $\text{OC}_2\text{H}_5$  –  $\text{OC}_{12}\text{H}_{25}$ <sup>25–41</sup> and  $\text{OC}_{14}\text{H}_{29}$  –  $\text{OC}_{18}\text{H}_{37}$ <sup>39,40,42–45</sup> appendages was required to enhance the stability of complex aggregates (also see ref 46). In addition, the  $\pi$ – $\pi$ , dipolar, and bromobonding interactions of 1,2-dibromo-4,5-dialkoxybenzenes, studied by Cukiernik et al.,<sup>42,47</sup> were utilized for assembly of our 4,5-dialkoxy “V”-type building blocks. This combination produced the desired “V”-monomers possessing  $-\text{OCH}_3$ ,  $-\text{OC}_6\text{H}_{13}$ ,  $-\text{OC}_{10}\text{H}_{21}$ ,  $-\text{OC}_{16}\text{H}_{33}$ , and  $-\text{OC}_{22}\text{H}_{45}$  moieties for the apex positions in the triangular constructs. These simple triangles opened a pathway for easy access to more complex motifs. In particular, as illustrated in Figure 1, the simple triangle **1a**, derived from three “V”-monomers with the  $-\text{OC}_{22}\text{H}_{45}$  chains<sup>48</sup> with precisely 3 equiv of “K”-monomer possessing the  $-\text{OCH}_3$  marker and 9 equiv of the same metal easily generated the desired larger Sierpiński triangle **1b**, as the initial sole product.

The established quantitative stoichiometric control exhibited in the construction of the initial Sierpiński triangle<sup>17</sup> provides the synthetic freedom to precisely control the size and shape of the resultant assemblies. Thus, the same monomers that generated the simple triangle (1:1; *bis* terpyridine to metal) and the G1 Sierpiński triangle (1:1:3; *bis* terpyridine to tetrakis terpyridine to metal) afforded a G2 Sierpiński triangle (1:4:9; *bis* terpyridine to tetrakis terpyridine to metal) (Figure 1a–c).

Received: January 30, 2020

Published: March 4, 2020

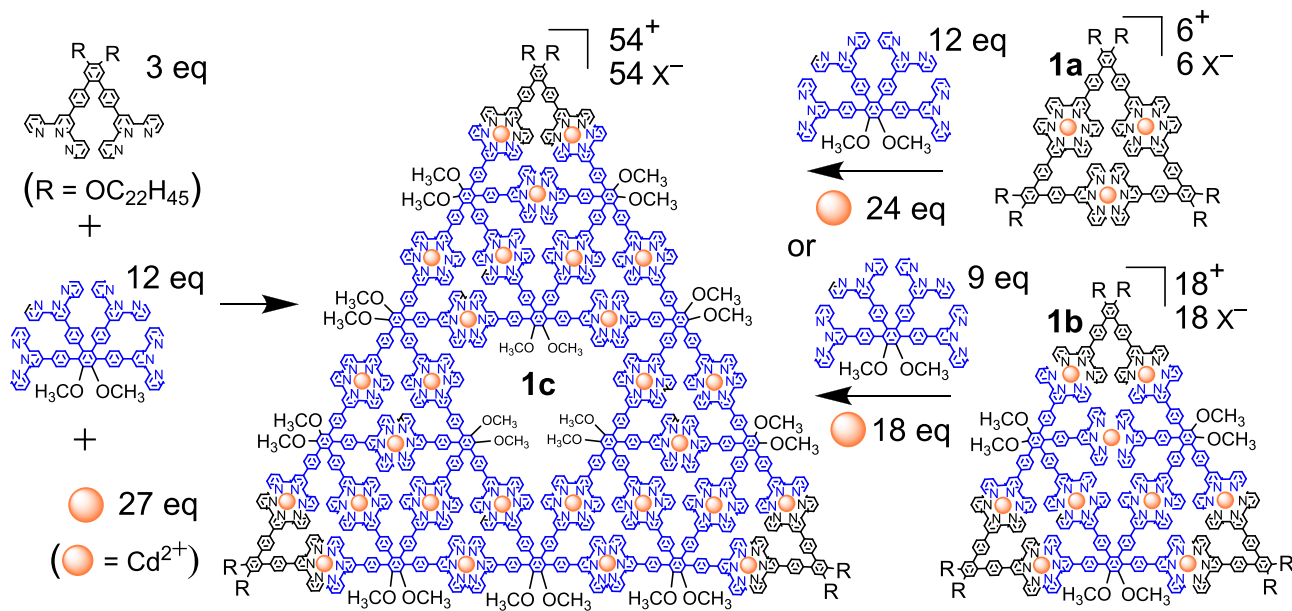


**Figure 1.** 2D Sierpiński triangle construction based on precise stoichiometry, complementary building block design, and metal-complex lability.

Notably, since the elementary trimer **1a** and G1 triangle **1b** are each composed to the requisite 60°-based, *bis* terpyridine, vertex-based monomers, and an already defined ratio of tetrakis terpyridine and metal, we anticipated the precise combination of trimer **1a** and G1 **1b** with tetrakis terpyridine and added metal (1:12:24 or 1:9:18, respectively) would self-assemble and generate the G2 triangle **1c**; the key to the process is the lability of the metal<sup>2+</sup> complex. The incorporation of the lipophilic alkyl chains at the vertices of the triangles offers the enhanced self-assembly and will be discussed below.

The alkylated, related G3 triangle was generated in 95% yield by a simple one-step, puzzle-like process.<sup>49</sup> The construction of a G2 Sierpiński triangle with two C<sub>16</sub> alkyl chains at the vertices and with -OCH<sub>3</sub> facial moieties, as spectral NMR markers, in the presence of Cd(NO<sub>3</sub>)<sub>2</sub>·4H<sub>2</sub>O (ratio 1:4:9) offers an opportunity to look for complex aggregates. The reaction sequence was repeated but using the longer C<sub>22</sub> alkyl moieties; however, attempts to analyze the resultant product(s) were frustrated by complicated NMR and mass spectra data that were contaminated with larger peaks. To ascertain additional data and further explore our results, imaging of these samples was conducted at the Nanotechnology Core Facility of the USFDA. TEM images (Figure 2a and 2b) revealed and suggested the formation of large triangular-shaped particles. The 3D AFM image of Figure 2b is shown in Figure 2c. The results show (Figure 2c) a sharp, crystalline-like, 3D structure, with the large structure possessing edge lengths in the 300–400 nm range and with a height of 150 nm; there is a clear polygon base and apex with each lateral base and apex forming a triangle. This is the description of a well-defined, triangular pyramid.

We have also performed detailed and coarse-grained molecular dynamics simulations to establish stability and possible pathways for assembly of the pyramidal structures (see Supporting Information (SI) for details). This was done to cover multiple length and time scales controlling the self-assembly process. In particular, Figure 3a, b present pyramid self-assembly driven by aggregation of the alkyl chains attached

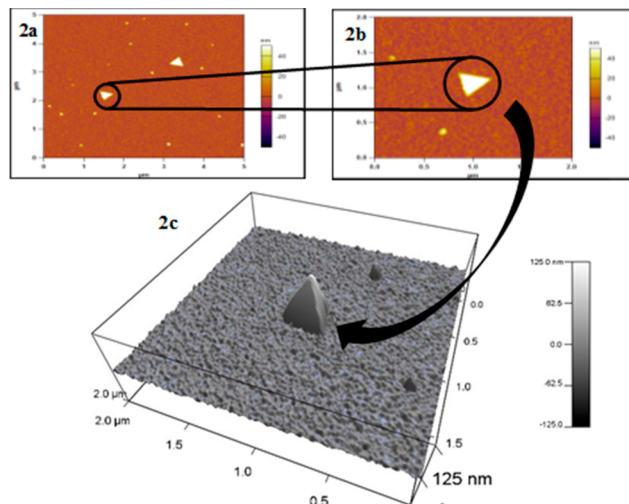


**Figure 2.** TEM of the third generation triangle (**2a**) and its close-up view (**2b**) and the corresponding 3D AFM image of its self-assembled pyramid (**2c**).

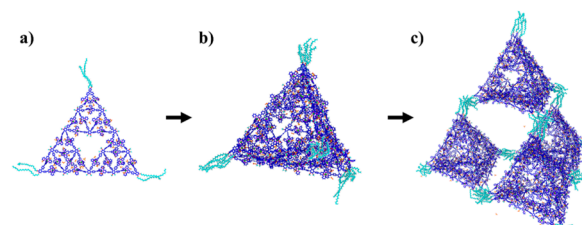


**Figure 3.** Simulation snapshots of G3 2D Sierpiński triangle (a); G1 3D pyramid structure (b); illustration of the possible multipyramid assembly (c), obtained by energy optimization of the preassembled multipyramid structure.

at corners of the 2D Sierpiński triangle **3a**. To establish the effect of alkyl chain length on the self-assembly process, we have performed multiscale molecular dynamics simulations (see SI). These simulations have shown that with increasing

length of the alkyl chains, the molecular pyramid framework is formed by the corner-to-corner assembly of four planar Sierpiński-type triangles (Figure 3a and Figure S2). The thermodynamic stability of such aggregates significantly improves with increasing the alkyl chain length. As we have shown in the SI, there exists a linear scaling relation between the energy difference required for separation of the triangular facet of the pyramid and the length of the alkyl chains forming aggregates at pyramid corners. Furthermore, the pyramids could continue to stack generating a higher-order, Sierpiński pyramid, based on highly ordered megastructures, as illustrated in Figure 3c. This is in agreement with the AFM image in Figure 2c displaying two high-definition, well-resolved, sharp triangles indicative of the ordered assembly of the G2 triangle 2c, whereas, a lateral, side-on view revealed a nearly perfect pyramidal structure (edge distance: 300 nm × height: 150 nm).

The potential to “glue” the connective lipophilic arms via a self-assembly process offers attractive possibilities for secondary aggregation scenarios. As well as tying these tiles together in a 3D manner, the potential to craft 2D materials is envisioned. The specific positioning of the sites of connectivity needs to be evaluated, since there can be vertex as well as facial connectivity, or both, based on different types of “strings”. Interactions of these tiles at the solvent–water interface will need to be evaluated for 2D patterning, and this can also be considered for molecular squares, based on Pd/Pt connectivity.

Protein self-assembly has become a powerful tool and inspiration for development of materials with advanced properties. Although the mechanism of assembly of the 3D viral pyramid is not yet fully elucidated, it does require the PVAP hydrophobic N-terminal transmembrane helix segment along with the C-terminal hydrophilic domains to form protein sheets that consist of two layers.<sup>1</sup> The spontaneous generation of these Sierpiński pyramids is demonstrated to occur via stacking of the Sierpiński triangles with molecular-directed intertwinement of the alkyl side chains. Essentially, these materials exhibit first-order assembly to generate a triangle followed by second-order assembly to give the higher architecture pyramids. Both mechanisms require identical subunits with different functional motifs within the monomer that dictate structural associations and creation of these three-dimensional aggregates.

## ASSOCIATED CONTENT

### Supporting Information

The Supporting Information is available free of charge at <https://pubs.acs.org/doi/10.1021/jacs.0c01168>.

Experimental and characterization details of all ligands and triangles, collision cross section data, TEM and AFM procedures, and detailed molecular modeling studies (PDF)

## AUTHOR INFORMATION

### Corresponding Authors

George R. Newkome — Department of Polymer Science and Department of Chemistry, The University of Akron, Akron, Ohio 44325, United States; Center for Molecular Biology and Biotechnology, Florida Atlantic University, Jupiter, Florida 33458, United States; [orcid.org/0000-0001-6019-5071](https://orcid.org/0000-0001-6019-5071); Email: newkome@fau.edu

Andrey V. Dobrynin — Department of Polymer Science, The University of Akron, Akron, Ohio 44325, United States; [orcid.org/0000-0002-6484-7409](https://orcid.org/0000-0002-6484-7409); Email: adobrynin@uakron.edu

Chrys Wesdemiotis — Department of Chemistry and Department of Polymer Science, The University of Akron, Akron, Ohio 44325, United States; [orcid.org/0000-0002-7916-4782](https://orcid.org/0000-0002-7916-4782); Email: wesdemiotis@uakron.edu

## Authors

Rajarshi Sarkar — Department of Polymer Science, The University of Akron, Akron, Ohio 44325, United States; [orcid.org/0000-0003-1281-7993](https://orcid.org/0000-0003-1281-7993)

Ting-Zheng Xie — Department of Polymer Science, The University of Akron, Akron, Ohio 44325, United States; [orcid.org/0000-0001-6717-7642](https://orcid.org/0000-0001-6717-7642)

Kevin J. Endres — Department of Polymer Science, The University of Akron, Akron, Ohio 44325, United States; [orcid.org/0000-0002-0857-6966](https://orcid.org/0000-0002-0857-6966)

Zilu Wang — Department of Polymer Science, The University of Akron, Akron, Ohio 44325, United States; [orcid.org/0000-0002-5957-8064](https://orcid.org/0000-0002-5957-8064)

Charles N. Moorefield — Dendronex LLC, Lubbock, Texas 79416, United States; [orcid.org/0000-0002-1197-9192](https://orcid.org/0000-0002-1197-9192)

Mary Jane Saunders — Department of Biological Sciences, Florida Atlantic University, Boca Raton, Florida 33431, United States

Suman Ghori — NCTR-ORA Nanotechnology Core Facility, National Center for Toxicological Research, U.S. Food & Drug Administration, Jefferson, Arkansas 72079, United States

Anil K. Patri — NCTR-ORA Nanotechnology Core Facility, National Center for Toxicological Research, U.S. Food & Drug Administration, Jefferson, Arkansas 72079, United States

Complete contact information is available at:  
<https://pubs.acs.org/10.1021/jacs.0c01168>

## Notes

The authors declare no competing financial interest.

## ACKNOWLEDGMENTS

The authors gratefully acknowledge the funding from the National Science Foundation (CHE-1151991 to G.R.N. and CHE-1808115 to C.W.) for the initial phases of this work and the James and Vanita Oelschlager funding via The University of Akron.

## REFERENCES

- (1) Daum, B.; Quax, T. E. F.; Sachse, M.; Mills, D. J.; Reimann, J.; Yıldız, Ö.; Häder, S.; Saveanu, C.; Forterre, P.; Albers, S.-V.; Kühlbrandt, W. Self-assembly of the general membrane-remodeling protein PVAP into sevenfold virus-associated pyramids. *Proc. Natl. Acad. Sci. U. S. A.* **2014**, *111*, 3829–3834.
- (2) Quax, T. E.; Lucas, S.; Reimann, J.; Pehau-Arnaudet, G.; Prevost, M. C.; Forterre, P.; Albers, S. V.; Prangishvili, D. Simple and elegant design of a virion egress structure in Archaea. *Proc. Natl. Acad. Sci. U. S. A.* **2011**, *108*, 3354–3359.
- (3) Snyder, J. C.; Brumfield, S. K.; Peng, N.; She, Q.; Young, M. J. Sulfolobus turreted icosahedral virus c92 protein responsible for the formation of pyramid-like cellular lysis structures. *J. Virol.* **2011**, *85*, 6287–6292.
- (4) Krzysztofik, W. J. Fractal Geometry in Electromagnetics Applications - from Antenna to Metamaterials. *Microwave Rev.* **2013**, Dec, 3–14.

- (5) Chen, L.-J.; Zhao, G.-Z.; Jiang, B.; Sun, B.; Wang, M.; Xu, L.; He, J.; Abiliz, Z.; Tan, H.; Li, X.; Yang, H.-B. Smart Stimuli-Responsive Spherical Nanostructures Constructed from Supramolecular Metalodendrimers via Hierarchical Self-Assembly. *J. Am. Chem. Soc.* **2014**, *136*, 5993–6001.
- (6) Samoc, M.; Corkery, T. C.; McDonagh, A. M.; Cifuentes, M. P.; Humphrey, M. G. Organometallic Complexes for Non-Linear Optics. 49. Third-Order Non-linear Optical Spectral Dependence Studies of Arylalkynylruthenium Dendrimers. *Aust. J. Chem.* **2011**, *64*, 1269–1273.
- (7) Chen, Y.-C.; Juang, T.-Y.; Dai, S. A.; Wu, T.-W.; Lin, J.-J.; Jeng, R.-J. Optical Non-Linearity from Montmorillonite Intercalated with a Chromophore-Containing Dendritic Structure: A Self-Assembly Approach. *Macromol. Rapid Commun.* **2008**, *29*, 587–592.
- (8) Benniston, A. C.; Harriman, A.; Pariani, C.; Sams, C. A. Intramolecular energy-transfer processes in a bis(porphyrin)-ruthenium(II) bis(2,2':6',2"-terpyridine) molecular array. *Phys. Chem. Chem. Phys.* **2006**, *8*, 2051–2057.
- (9) Rieth, S.; Hermann, K.; Wang, B.-Y.; Badjić, J. D. Controlling the dynamics of molecular encapsulation and gating. *Chem. Soc. Rev.* **2011**, *40*, 1609–1622.
- (10) Chen, Z.; Guo, B.; Yang, Y.; Cheng, C. Metamaterials-based enhanced energy harvesting: A review. *Phys. B* **2014**, *438*, 1–8.
- (11) Dai, L. *Intelligent Macromolecules for Smart Devices: From Materials Synthesis to Device Applications*; Springer-Verlag: London, 2004.
- (12) Yoshizawa, M.; Klosterman, J. K.; Fujita, M. Functional Molecular Flasks: New Properties and Reactions within Discrete, Self-Assembled Hosts. *Angew. Chem., Int. Ed.* **2009**, *48*, 3418–3438.
- (13) Rebek, J., Jr. Simultaneous Encapsulation: Molecules Held at Close Range. *Angew. Chem., Int. Ed.* **2005**, *44*, 2068–2078.
- (14) Fujita, D. Challenges to large molecular encapsulation. *Pure Appl. Chem.* **2014**, *86*, 3–11.
- (15) Lu, X.; Li, X.; Cao, Y.; Schultz, A.; Wang, J.-L.; Moorefield, C. N.; Wesdemiotis, C.; Cheng, S. Z. D.; Newkome, G. R. Self-Assembly of a Supramolecular, Three-Dimensional, Spoked, Bicycle-like Wheel. *Angew. Chem., Int. Ed.* **2013**, *52*, 7728–7731.
- (16) Lu, X.; Li, X.; Guo, K.; Xie, T.-Z.; Moorefield, C. N.; Wesdemiotis, C.; Newkome, G. R. Probing the Hidden World of Molecular Self-assembly: Concentration-dependent, Three-dimensional Supramolecular Interconversions. *J. Am. Chem. Soc.* **2014**, *136*, 18149–18155.
- (17) Sarkar, R.; Guo, K.; Moorefield, C. N.; Saunders, M. J.; Wesdemiotis, C.; Newkome, G. R. One-Step Multicomponent Self-Assembly of a First-Generation Sierpiński Triangle: From Fractal Design to Chemical Reality. *Angew. Chem., Int. Ed.* **2014**, *53*, 12182–12185.
- (18) Sarkar, R.; Guo, Z.; Li, J.; Burai, T. N.; Moorefield, C. N.; Wesdemiotis, C.; Newkome, G. R. Multicomponent reassembly of terpyridine-based materials: quantitative metallomacrocyclic rearrangement. *Chem. Commun.* **2015**, *51*, 12851–12864.
- (19) Li, Y.; Jiang, Z.; Yuan, J.; Wu, T.; Moorefield, C. N.; Newkome, G. R.; Wang, P. Facile thermodynamic conversion of a linear metallopolymer into a self-assembled hexameric metallomacrocycle. *Chem. Commun.* **2015**, *51*, 5766–5769.
- (20) Wei, C.; He, Y.; Shi, X.; Song, Z. Terpyridine-metal complexes: Applications in catalysis and supramolecular chemistry. *Coord. Chem. Rev.* **2019**, *385*, 1–19.
- (21) Chen, M.; Wang, J.; Wang, S.-C.; Jiang, Z.; Liu, D.; Liu, Q.; Zhao, H.; Yan, J.; Chan, Y.-T.; Wang, P. Truncated Sierpiński Triangular Assembly from a Molecular Mortise-Tenon Joint. *J. Am. Chem. Soc.* **2018**, *140*, 12168–12174.
- (22) Wang, S.-Y.; Huang, J.-Y.; Liang, Y.-P.; He, Y.-J.; Chen, Y.-S.; Zhan, Y.-Y.; Hiraoka, S.; Liu, Y.-H.; Peng, S.-M.; Chan, Y.-T. Multicomponent Self-Assembly of Metallo-Supramolecular Macrocycles and Cages through Dynamic Heteroleptic Terpyridine Complexation. *Chem. - Eur. J.* **2018**, *24*, 9274–9284.
- (23) Xie, T.-Z.; Wu, X.; Endres, K. J.; Guo, Z.; Lu, X.; Li, J.; Manandhar, E.; Ludlow, J. M., III; Moorefield, C. N.; Saunders, M. J.; Wesdemiotis, C.; Newkome, G. R. Supercharged, Precise, Megametalodendrimers via a Single-Step, Quantitative, Assembly Process. *J. Am. Chem. Soc.* **2017**, *139*, 15652–15655.
- (24) Roberts, D. A.; Pilgrim, B. S.; Sirvinskaite, G.; Ronson, T. K.; Nitschke, J. R. Covalent Post-assembly Modification Triggers Multiple Structural Transformations of a Tetrazine-Edged  $\text{Fe}_4\text{L}_6$  Tetrahedron. *J. Am. Chem. Soc.* **2018**, *140*, 9616–9623.
- (25) He, Q.; Yang, J.; Lin, H.; Zhang, L.; Song, Y.; Bai, F. Synthesis, Characterization and *Cis*-*Trans* Photoisomerization of a Series of Hyperbranched Conjugated Polymers. *Polym. Adv. Technol.* **2003**, *14*, 297–302.
- (26) Ris, D. P.; Schneider, G. E.; Ertl, C. D.; Kohler, E.; Müntener, T.; Neuburger, M.; Constable, E. C.; Housecroft, C. E. 4'-Functionalized 2,2':6',2"-terpyridines as the  $\text{NN}$  domain in  $[\text{Ir}(\text{CN})_2(\text{NN})]\{\text{PF}_6\}$  complexes. *J. Organomet. Chem.* **2016**, *812*, 272–279.
- (27) Klein, Y. M.; Prescimone, A.; Constable, E. C.; Housecroft, C. E. 2-Dimensional networks assembled using 4'-functionalized 4,2':6',4"-terpyridines and  $\text{Co}(\text{NCS})_2$ . *Polyhedron* **2016**, *103*, 58–65.
- (28) Wu, N.-W.; Chen, L.-J.; Wang, C.; Ren, Y.-Y.; Li, X.; Xu, L.; Yang, H.-B. Hierarchical self-assembly of a discrete hexagonal metallacycle into the ordered nanofibers and stimuli-responsive supramolecular gels. *Chem. Commun.* **2014**, *50*, 4231–4233.
- (29) Ren, Y.-Y.; Xu, Z.; Li, G.; Huang, J.; Fan, X.; Xu, L. Hierarchical self-assembly of a fluorescence emission-enhanced organogelator and its multiple stimuli-responsive behaviors. *Dalton Trans.* **2017**, *46*, 333–337.
- (30) Klein, Y. M.; Constable, E. C.; Housecroft, C. E.; Zampese, J. A.; Crochet, A. Greasy tails switch 1D-coordination  $[\{\text{Zn}_2(\text{OAc})_4(4'-(4-\text{ROC}_6\text{H}_4)-4,2':6',4"-tpy)\}_2]$  polymers to discrete  $[\{\text{Zn}_2(\text{OAc})_4(4'-(4-\text{ROC}_6\text{H}_4)-4,2':6',4"-tpy)\}_2]$  complexes. *CrystEngComm* **2014**, *16*, 9915–9929.
- (31) Constable, E. C.; Housecroft, C. E.; Vujovic, S.; Zampese, J. A. 2D  $\rightarrow$  2D Parallel interpenetration of (4,4) sheets constructed from a ditopic bis(4,2':6',4"-terpyridine). *CrystEngComm* **2014**, *16*, 3494–3497.
- (32) Klein, Y. M.; Constable, E. C.; Housecroft, C. E. A 3-dimensional  $\{4^2.8^4\}$  lvt net built from a ditopic bis(3,2':6',3"-terpyridine) tecton bearing long alkyl tails. *CrystEngComm* **2015**, *17*, 2070–2073.
- (33) Klein, Y. M.; Prescimone, A.; Constable, E. C.; Housecroft, C. E. Manipulating connecting nodes through remote alkoxy chain variation in coordination networks with 4'-alkoxy-4,2':6',4"-terpyridine linkers. *CrystEngComm* **2015**, *17*, 6483–6492.
- (34) Klein, Y. M.; Prescimone, A.; Neuburger, M.; Constable, E. C.; Housecroft, C. E. What a difference a tail makes: 2D - 2D parallel interpenetration of sheets to interpenetrated nbo networks using ditopic-4,2':6',4"-terpyridine ligands. *CrystEngComm* **2017**, *19*, 2894–2902.
- (35) Vujovic, S.; Constable, E. C.; Housecroft, C. E.; Morris, C. D.; Neuburger, M.; Prescimone, A. Engineering 2D - 3D parallel interpenetration using long alkoxy-chain substituents. *Polyhedron* **2015**, *92*, 77–83.
- (36) Cheng, K.-Y.; Wang, S.-C.; Chen, Y.-S.; Chan, Y.-T. Self-Assembly and Catalytic Reactivity of BINOL-Bridged Bis(phenanthroline) Metallocages. *Inorg. Chem.* **2018**, *57*, 3559–3567.
- (37) Wang, L.; Zhang, Z.; Jiang, X.; Irvin, J. A.; Liu, C.; Wang, M.; Li, X. Self-Assembly of Tetrameric and Hexameric Terpyridine-Based Macrocycles Using  $\text{Cd}(\text{II})$ ,  $\text{Zn}(\text{II})$ , and  $\text{Fe}(\text{II})$ . *Inorg. Chem.* **2018**, *57*, 3548–3558.
- (38) Zhang, Y.; Zhou, Q.-F.; Huo, G.-F.; Yin, G.-Q.; Zhao, X.-L.; Jiang, B.; Tan, H.; Li, X.; Yang, H.-B. Heirarchical Self-Assembly of an Alkynylplatinum(II) Bzimpy-Functionalized Metallacage via  $\text{Pt}\cdots\text{Pt}$  and  $\pi\cdots\pi$  Interactions. *Inorg. Chem.* **2018**, *57*, 3516–3520.
- (39) Yuan, Y.; Li, J.; He, L.; Zhang, H. Influence of alkoxy tail length on the properties of side chain liquid crystal polymers with aggregation-induced emission enhancement characteristics. *Eur. Polym. J.* **2018**, *105*, 7–16.

- (40) Li, Y.; Tatum, W. K.; Onorato, J. W.; Zhang, Y.; Luscombe, C. K. Low Elastic Modulus and High Charge Mobility of Low-Crystallinity Indacenodithiophene-Based Semiconducting Polymers for Potential Applications in Stretchable Electronics. *Macromolecules* **2018**, *51*, 6352–6358.
- (41) Ai, Y.; Ng, M.-K.; Hong, E. Y.-H.; Chan, A. K.-W.; Wei, Z.-W.; Li, Y.; Yam, V. W.-W. Solvent-Induced and Temperature-Promoted Aggregation of Bipyridine Platinum(II) Triangular Metallacycles and their Near-Infrared Emissive Behaviours. *Chem. - Eur. J.* **2018**, *24*, 11611–11618.
- (42) Fonrouge, A.; Cecchi, F.; Albores, P.; Baggio, R.; Cukiernik, F. D. Relative influence of noncovalent interactions on the melting points of a homologous series of 1,2-dibromo-4,5-dialkoxybenzenes. *Acta Crystallogr., Sect. C: Cryst. Struct. Commun.* **2013**, *C69*, 204–208.
- (43) Würthner, F.; Thalacker, C.; Sautter, A. Hierarchical Organization of Functional Perylene Chromophores to Mesoscopic Superstructures by Hydrogen Bonding and  $\pi$ - $\pi$  Interactions. *Adv. Mater.* **1999**, *11*, 754–758.
- (44) Roy, S.; Hazra, A.; Bandyopadhyay, A.; Raut, D.; Madhusri, P. L.; Rao, D. S. S.; Ramamurty, U.; Pati, S. K.; Prasad, S. K.; Majji, T. K. Reversible Polymorphism, Liquid Crystallinity, and Stimuli-Responsive Luminescence in a Bola-amphiphilic  $\pi$ -System: Structure-Property Correlations Through Nanoindentation and DFT Calculations. *J. Phys. Chem. Lett.* **2016**, *7*, 4086–4092.
- (45) Yao, Y.; Chakraborty, S.; Zhu, S.; Endres, K. J.; Xie, T.-Z.; Hong, W.; Manandhar, E.; Moorefield, C. N.; Wesdemiotis, C.; Newkome, G. R. Stepwise, multicomponent assembly of a molecular trapezoid possessing three different metals. *Chem. Commun.* **2017**, *53*, 8038–8041.
- (46) Barbon, S. M.; Rolland, M.; Anastasaki, A.; Truong, N. P.; Schulze, M. W.; Bates, C. M.; Hawker, C. J. Macrocyclic Side-Chain Monomers for Photoinduced ATRP: Synthesis and Properties versus Long-Chain Linear Isomers. *Macromolecules* **2018**, *51*, 6901–6910.
- (47) Cukiernik, F. D.; Zelcer, A.; Garland, M. T.; Baggio, R. Halogen bonding in 1,2-dibromo-4,5-dimethoxybenzene and 1,2-diido-4,5-dimethoxybenzene. *Acta Crystallogr., Sect. C: Cryst. Struct. Commun.* **2008**, *64*, o604–o608.
- (48) Xie, T.-Z.; Yao, Y.; Sun, X.; Endres, K. J.; Zhu, S.; Wu, X.; Li, H.; Ludlow, J. M., III; Liu, T.; Gao, M.; Moorefield, C. N.; Saunders, M. J.; Wesdemiotis, C.; Newkome, G. R. Supramolecular Arrays by Self-Assembly of Terpyridine-Based Monomers and Transition Metal Ions. *Dalton Trans.* **2018**, *47*, 7528–7533.
- (49) Jiang, Z.; Li, Y.; Wang, M.; Liu, D.; Yuan, J.; Chen, M.; Wang, J.; Newkome, G. R.; Sun, W.; Li, X.; Wang, P. Constructing High-generation Sierpiński Triangles by Molecular Puzzling. *Angew. Chem., Int. Ed.* **2017**, *56*, 11450–11455.